Bull. Soc. R. Sci. Liège, 2024, **93**(2), 738–751 *Peer-reviewed conference paper*
doi:10.25518/0037-9565.11863

Intranight Variability of Ultraviolet Emission From High-z Blazars

Krishan CHAND[1,2]

[1] Aryabhatta Research Institute of Observational Sciences (ARIES), Manora Peak, Nainital–263002, India
[2] Now at: Department of Physics and Astronomical Science, Central University of Himachal Pradesh (CUHP), Dharamshala–176215, India
Correspondence to: krishanchand.kc007@gmail.com

Paper presented at the 3rd BINA Workshop on "Scientific Potential of the Indo-Belgian Cooperation", held at the Graphic Era Hill University, Bhimtal (India), 22nd–24th March 2023.

Abstract

Rapid intranight variability of continuum and polarization in blazars is a valuable tool for probing the beaming of a relativistic jet and the associated population of the relativistic particles. Although such intranight variability in the rest-frame optical continuum has been extensively studied, there is a scarcity in the rest-frame ultraviolet (UV), where the variability might be caused by a secondary population of relativistic particles. To address this gap, we recently reported, for the first time, an intranight variability study of a sample of high-z blazars (Chand et al., 2022), with the monitored optical radiation is being their rest-frame UV radiation. Here, we discuss in detail the implications of this investigation, including a proper comparison of high-z blazar samples with fractional optical polarization ($p_{\rm opt}$) lower and greater than 3%. In this context, we also report an intranight variability study of an additional high-z blazar at $z = 2.347$, namely J161942.38+525613.41, monitored over three sessions, each lasting approximately five hours. Our investigation does not reveal any compelling evidence for a stronger intranight variability of the UV emission in high polarization blazars, in contrast to the blazars monitored in the rest-frame blue-optical. We also discuss this trend in the light of the suggestion that the synchrotron radiation of blazar jets in the UV/X-ray regime may arise from a relativistic particle population different from that radiating up to near-infrared/optical frequencies.

Keywords: galaxies: active, galaxies: photometry, galaxies: high-redshift, galaxies

1. Introduction

Blazars are radio-loud Active Galactic Nuclei (AGN) whose radiation is predominantly non-thermal. The source of their radiation is a relativistic jet that is approximately aligned with the observer's line of sight and thus beamed toward the observer (Blandford and Rees, 1978; Moore and Stockman, 1984; Urry and Padovani, 1995). This radiation appears highly Doppler boosted in the direction of the observer due to beaming, completely dominating the

radiation from the host galaxy and the accretion disk. Rapid variability of continuum and polarized emission, along with a flat radio spectrum (i.e., a dominant radio core), are well-known characteristics of this beaming phenomenon. The quasar subset of blazars with higher power, known as flat-spectrum radio quasars (FSRQs) exhibit these characteristics (see, e.g., Stockman et al., 1984; Wills et al., 1992; Angelakis et al., 2016). Their jets frequently exhibit superluminal motion and variability amplitudes at all wavelengths, from radio to γ-rays. The flux variability observed from radio to optical and even TeV bands has been instrumental in elucidating the physics of blazars, particularly the extreme cases of flux variability observed on time scales of hours or even shorter (e.g., Wagner and Witzel, 1995; Aharonian et al., 2017; Gopal-Krishna and Wiita, 2018).

The UV band is an important spectral region for which little information about intranight variability is available. The primary reason for the lack of information about the rapid UV variability of AGN is that intranight monitoring campaigns for space-borne UV telescopes are prohibitively time-consuming, although attempts have been made to fill this information gap by using UV data acquired with GALEX for large AGN samples in recent years. However, such studies covered only day-like or longer time scales and were particularly focused on optically selected quasars (e.g., Punsly et al., 2016; Xin et al., 2020). Hence, these studies may have had substantial contributions from the accretion disk and may not have measured only UV emission of synchrotron origin. Additionally, from detailed measurements of the spectral energy distribution (SED) of a few quasar jets, a hint regarding UV radiation has emerged, suggesting that a very substantial, if not dominant, contribution to synchrotron UV radiation from quasar jets may arise from a relativistic particle population distinct from the one responsible for their radiation up to near-infrared and optical frequencies. Specifically, the SED of the knots in the kiloparsec-scale radio jets of some quasars exhibits a sharp spectral *upturn* towards the UV and connects smoothly thereafter to the X-ray data points (Uchiyama et al., 2006, 2007; Jester et al., 2007). Moreover, the observed high polarization in the UV emission supports a synchrotron interpretation for this higher-energy radiation component (Cara et al., 2013). The studies mentioned above support the idea that the optical and UV radiations from jets are synchrotron radiation arising from two different populations of relativistic particles. This idea was recently reinforced by Chand et al. (2022) who compared the intranight flux variability of blazars at the rest-frame UV and optical wavelengths.

To investigate the rapid UV variability of blazars, Chand et al. (2022) adopted a practical approach, conducting intranight *optical* monitoring of 14 blazars (FSRQs) located at very high redshifts ($1.5 < z < 3.7$), so that their monitored optical radiation was actually UV emission in the rest-frame. Their study focused on two prominent subclasses of blazars distinguished by low and high fractional polarization measured in the optical, with the separation limit set at $p_{\rm opt} = 3\%$ (Moore and Stockman, 1984). This provided a set of nine low-polarization FSRQs, with $p_{\rm opt} < 3\%$, and five high-polarization FSRQs, with $p_{\rm opt} > 3\%$. Based on photometric statistical analysis for these nine low- and five high-polarization FSRQs, they found no evidence for a strong correlation of intranight variability of UV emission and polarization, in contrast to the strong correlation found for intranight variability of optical emission. This led them to propose that the synchrotron radiation of blazar jets in the UV/X-ray regime arises from a relativistic

particle population distinct from the one responsible for their synchrotron radiation up to near-infrared/optical frequencies. However, since their two samples are too small to be representative of the high-z blazar population, this finding might be spurious. Therefore, independent verification on this finding is required. This can be achieved through intranight optical monitoring of a larger sample of high-z blazars with low and high polarization. To enhance the statistical robustness of the above finding, we focused on a sample of 34 high-z blazars, which is 2.4 times larger than the combined sample of low-and high-polarization blazars of Chand et al. (2022) (see Sect. 2). The main obstacle in enlarging the sample of high-z blazars to study the intranight variability of rest-frame UV emission with polarization is the lack of polarization information in the literature. It is essential to have high-z blazars with both low and high polarization to explore the dependence of intranight UV variability with polarization. More than half of the sources (19) in our sample of 34 high-z blazars furthermore lack polarization information in the literature. Therefore, the purpose of the intranight variability study of the UV emission for our sample of high-z blazars is twofold: (i) obtaining polarization measurements of the sources, and (ii) conducting intranight optical monitoring of the sources. The selected 34 high-z blazars have a brightness (m_R) range from 15.2 to 17.4 and detecting polarization of a few per cent within this brightness range requires telescopes with diameter of at least 2–3 m. Therefore, for polarization measurements, we are submitting proposals in anticipation of the availability of an imaging polarimeter at the 3.6-m Devasthal Optical Telescope (DOT) at ARIES, while intranight optical monitoring will be carried out using metre-class telescopes available in India.

The polarization and intranight optical observations for high-z blazar samples in Chand et al. (2022) are separated by a median time of four years. Fluctuations in the polarization state of about a quarter of FSRQs on a year-like time scale has been reported in various studies (Impey and Tapia, 1990; Chand and Gopal-Krishna, 2022; Chand et al., 2023). Due to the variable nature of polarization for blazars, quasi-simultaneous observations of both polarimetry and photometry are desirable. However, conducting both types of observations simultaneously is quite challenging. It is worth noting that a strong correlation exists between intranight optical variability (INOV) and $p_{\rm opt}$ for moderately distant blazars, despite the fact that the two sets of observations were made a decade apart (Goyal et al., 2012, and references therein). It is furthermore known that long-term optical variability is stronger for sources with large $p_{\rm opt}$ (e.g., Angelakis et al., 2016). Therefore, it would be beneficial not only to enlarge the sample of high-z blazars for studying the intranight variability of the UV continuum, but also to conduct intranight photometric observations concurrently with quasi-simultaneous polarimetric observations. This serves as the main motivation of this article, where we devise a large sample of 34 high-z blazars for intranight variability and quasi-simultaneous polarimetric observations, based on the upcoming imaging polarimeter at the 3.6-m DOT. As part of this ongoing long-term project, we present intranight optical monitoring of one of the 34 high-z blazars, namely J161942.38+525613.41 at $z = 2.347$, in three sessions with a median duration of ~ 5 h.

The article is organised as follows. In Sect. 2, we present a selection of an enlarged sample of high-z blazars along with notes on J161942.38+525613.41. Section 3 provides details about the photometric monitoring and data reduction, while the statistical analysis is briefly presented in Sect. 4. Finally, we offer a detailed discussion and draw conclusions in Sect. 5.

2. The Enlarged Sample of High-z Blazars

The enlarged sample of high-z blazars for intranight optical and polarimetric monitoring was selected from the 3561 sources listed in the fifth edition of the *Roma* Blazar catalogue (*Roma–BZCAT*, Massaro et al., 2015). These sources are either confirmed blazars or exhibit blazar-like characteristics. The redshift requirement of $z > 1.5$ was first applied to the 3651 sources. 784 blazars met this criterion. Subsequently, a brightness filter, $m_R < 17.5$, was applied to these 784 blazars to ensure a good signal-to-noise ratio (SNR) with metre-class telescopes, resulting in 84 blazars. However, 41 of these were discarded due to their negative declinations, and an additional nine sources were omitted to the impossibility of conducting long intranight monitoring sessions during the monsoon period, when these sources transit at night. The final enlarged sample of high-z blazars thus consists of 34 sources with redshift $z > 1.5$. Among these 34 blazars, nine sources were previously reported in Chand et al. (2022). In this article, we present the INOV results for one of the 34 high-z blazars, namely J161942.38+525613.41, alongside previously reported results for blazars in Chand et al. (2022). Below, we provide notes on this particular source.

J161942.38+525613.41 is classified as an FSRQ type of blazar with a brightness (m_R) of 16.7 mag (Massaro et al., 2015). It is located at a redshift of 2.347 (Peña-Herazo et al., 2021) with a logarithmic bolometric luminosity of 47.78 erg s^{-1} (Rakshit et al., 2020), placing it in the high-luminosity tail of blazars. The source has been detected in radio bands with a flux density of 182 mJy at 1.4 GHz (Condon et al., 1998) and 128 mJy at 5 GHz (Gregory et al., 1996). A flat radio spectral index (α_r) of -0.07 (Bourda et al., 2010) signifies the core dominance of the source. Due to its high redshift of 2.347, the monitored optical radiation actually represents rest-frame UV emission. Rakshit et al. (2020) estimated its logarithmic continuum luminosities to be 47.19 erg s^{-1} at 1350 Å and 46.84 erg s^{-1} at 3000 Å.

3. Photometric Monitoring and Data Reduction

For the high-z FSRQ J161942.38+525613.41 ($z = 2.347$), we conducted intranight photometric observations in the Johnson–Cousins R or SDSS r-band during three sessions, each with a median duration of 5.06 h. The observations were carried out using two telescopes: the 1.04-m Sampuranand Telescope (ST; Sagar, 1999), utilized for two sessions, and the 3.6-m Devasthal Optical Telescope (DOT; Kumar et al., 2018), employed for one session. For the ST sessions, observations were performed with a 4K $\times$ 4K CCD fixed at the focal plane of the Ritchey–Chrétien (RC) type telescope (Sagar, 1999). The 4K $\times$ 4K CCD was cooled to -120 °C using liquid nitrogen to minimise dark noise. With a pixel size of 15 microns and a plate scale of 0.23 arcsec per pixel, the CCD covered a field of view (FOV) of 15×15 arcmin^2 on the sky. Observations were conducted in 4×4 binning mode at a gain of 3 e$^-$ per analog-to-digital unit (ADU) and a readout speed of 1 MHz, with a readout noise of 7 e$^-$. For the DOT session, observations were carried out with the ARIES Devasthal–Faint Object Spectrograph and Camera (ADFOSC) mounted at the Cassegrain main port of the Ritchey–Chrétien (RC) designed telescope (Kumar et al., 2018). ADFOSC is equipped with a deep depletion 4K $\times$ 4K CCD, cooled to -120 °C using a closed-cycle cryo-cooling thermal engine. With a pixel size of 15 microns

Table 1: Basic parameters of the selected comparison stars (S1, S2, S3, S4) for the high-z blazar J161942.38+525613.41 (P). The comparison stars marked with * on a particular session have been utilized to determine the intranight optical variability (INOV) status of J161942.38+525613.41 (P).

Object	Date (yyyy/mm/dd)	R.A. (J2000) (hh:mm:ss)	Dec. (J2000)	g (mag)	r (mag)	$(g-r)$ (mag)
P	2020/04/21	16:19:42.38	+52°56′13.41″	16.82	16.74	0.08
	2020/04/25					
	2021/03/02					
S1	2020/04/21*	16:19:32.72	+52°49′35.19″	16.41	15.53	0.88
	2020/04/25*					
S2	2020/04/21	16:19:48.69	+52°58′19.60″	16.05	15.37	0.68
	2020/04/25*					
	2021/03/02*					
S3	2020/04/21*	16:19:37.29	+52°58′44.68″	15.92	15.33	0.59
	2020/04/25					
	2021/03/02*					
S4	2021/03/02	16:20:14.60	+52°52′17.80″	16.36	15.88	0.48

and a plate scale of ~ 0.2 arcsec per pixel, ADFOSC covered a FOV of 13.6×13.6 arcmin^2 on the sky (Omar et al., 2019). Observations were also carried out in 4×4 binning mode, with a readout noise of 8 e$^-$ at a speed of ~ 0.2 MHz and a gain of 1 e$^-$ per ADU.

The pre-processing of the raw images, which includes bias subtraction, flat-fielding and cosmic ray removal, was performed using standard tasks available in the Image Reduction and Analysis Facility (IRAF). Instrumental magnitudes of the target source and three selected comparison stars in the CCD frames were determined using aperture photometry (Stetson, 1987, 1992), with the Dominion Astronomical Observatory Photometry II (DAOPHOT II) algorithm. The aperture radius, a critical parameter for photometry, was determined by averaging the full width at half maximum (FWHM) of the point spread function (PSF) of five moderately bright stars. In this study, we fixed the aperture radius equal to twice the PSFs' average FWHM since the SNR was found to be highest for this aperture (see Chand et al., 2022). Subsequently, we derived differential light curves (DLCs) for the target source relative to the three selected comparison stars in the same CCD frames, which were within 1.5 magnitudes of the target source (see Table 1).

4. Statistical Analysis

In the current analysis, we utilized the F_η test to determine the presence of INOV in the derived DLCs (Chand et al., 2022; Gopal-Krishna et al., 2023). We further identified the two most stable comparison stars out of the three initially selected for each session. We then applied the F_η test to the three DLCs involving only these two stars. The selected two comparison

stars for each session are indicated within parentheses in column (4) of Table 2, and the corresponding DLCs are also labelled within parentheses in Fig. 1 on the right side. In various independent studies, it has been observed that the photometric errors returned by DAOPHOT are often too small (Gopal-Krishna et al., 1995; Garcia et al., 1999; Sagar et al., 2004; Stalin et al., 2004; Bachev et al., 2005; Goyal et al., 2012, 2013a). Consequently, the best value for the underestimation factor η has been found to be 1.54 ± 0.05, based on 262 monitoring sessions of quasars/blazars (Goyal et al., 2013b). We adopted the same value in this study. The F values for the selected two blazar DLCs in a given session are

$$F_1^{\eta} = \frac{\mathrm{Var}(q-s_1)}{\eta^2 \sum_{i=1}^{N} \sigma_{i,\mathrm{err}}^2 (q-s_1)/N}, \quad \text{and} \quad F_2^{\eta} = \frac{\mathrm{Var}(q-s_2)}{\eta^2 \sum_{i=1}^{N} \sigma_{i,\mathrm{err}}^2 (q-s_2)/N}, \tag{1}$$

where $\mathrm{Var}(q-s_1)$ and $\mathrm{Var}(q-s_2)$ are the variances of the target source relative to star 1 and star 2, respectively, $\sigma_{i,\mathrm{err}}^2(q-s_1)$ and $\sigma_{i,\mathrm{err}}^2(q-s_2)$ denote the errors returned by DAOPHOT for each individual data point of the target source relative to star 1 and star 2, respectively, N represents the total number of data points taken in the observation (column (2) of Table 2) and $\eta = 1.54$ is the scaling factor, as mentioned above. The computed F_1^{η} and F_2^{η} for the target source–star DLCs are reported in column (4) of Table 2.

The F values estimated from the $F_{1,2}^{\eta}$ test (column (4) of Table 2) are compared with the critical value of F (F_{c}^{α}) for $\alpha = 0.05, 0.01$ corresponding to confidence levels of 95% and 99%, respectively (columns (5) and (6) in Table 2). If the computed F value exceeds the critical value, the null hypothesis (i.e., no variability) is rejected. We thus classify a source for which F value $\geq F_{\mathrm{c}}(0.99)$ as *variable* ('V') at a confidence level ≥ 0.99; it is classified as *probable variable* ('PV') if $F_{\mathrm{c}}(0.95) < F$ value $< F_{\mathrm{c}}(0.99)$ and as *non-variable* ('NV') if the computed F value is less than $F_{\mathrm{c}}(0.95)$. In the F_{η} test where two F values are involved for comparison stars 1 and 2, we set the class of a target source as variable ('V') if the F value calculated for both source–star 1 and source–star 2 DLCs exceeds $F_{\mathrm{c}}(0.99)$; the target source is considered as non-variable ('NV') if the F value for at least one of the source-star DLCs is less than the $F_{\mathrm{c}}(0.95)$. For other remaining situations, i.e., a combination of V, PV or PV, PV, the target source is classified as a probable variable ('PV'). Column (9) of Table 2 lists the "Photometric Noise Parameter" (PNP), defined as PNP $= \sqrt{\eta^2 \langle \sigma_{i,\mathrm{err}}^2 \rangle}$, estimated for a monitoring session using the star–star DLCs, where $\eta = 1.54$, as mentioned above.

To enhance the credibility of the variability results, we attempted to derive the DLCs using the same set of three comparison stars (S1, S2, and S3) for the two observation sessions with the ST and for the single DOT session on April 21, 2020, April 25, 2020, and March 02, 2021, respectively. However, due to the lack of steadiness of S1 during the DOT session on March 02, 2021, a new stable comparison star, S4, was used instead of S1. Since the F_{η} test involves two comparison stars, we further identified the two most stable comparison stars out of the three for each session. We found a set of stable comparison stars (S1, S2, and S3) in different combinations for each of the two ST sessions and the DOT session (see Table 2, and also Fig. 1). Upon examining Fig. 1, it appears evident that there are significant variations on the first night and a good chance that there are some on the second night, but there is little chance of real variability on the third night, except perhaps for a slow rise and fall. However, the

Table 2: Results of the statistical test for detecting INOV in the DLCs of J161942.38+525613.41, where V = variable (confidence ≥ 0.99), PV = probable variable (confidence (0.95–0.99)), and NV = non-variable (confidence < 0.95).

Date	N	T	F-**test**			**INOV**			$\overline{\psi}$
(yyyy/mm/dd)		**(hr)**	F_1^η, F_2^η	F_c**(0.95)**	F_c**(0.99)**	**status**[a]		$\sqrt{\eta^2\langle\sigma^2_{i,err}\rangle}$	**(%)**
(1)	**(2)**	**(3)**	**(4)**	**(5)**	**(6)**	**(7)**	**(8)**	**(9)**	**(10)**
2020/04/21	51	4.97	1.83 (S1), 1.78 (S3)	1.60	1.95	PV , PV	PV	0.015 (S1-S3)	29.60
2020/04/25	58	5.06	0.60 (S1), 0.62 (S2)	1.55	1.87	NV , NV	NV	0.037 (S1-S2)	—
2021/03/02	138	5.47	6.63 (S2), 9.62 (S3)	1.33	1.49	V , V	V	0.005 (S2-S3)	15.89

[a] The variability status identifiers (column (7)) based on AGN–star1 and AGN–star2 DLCs are separated by a comma.

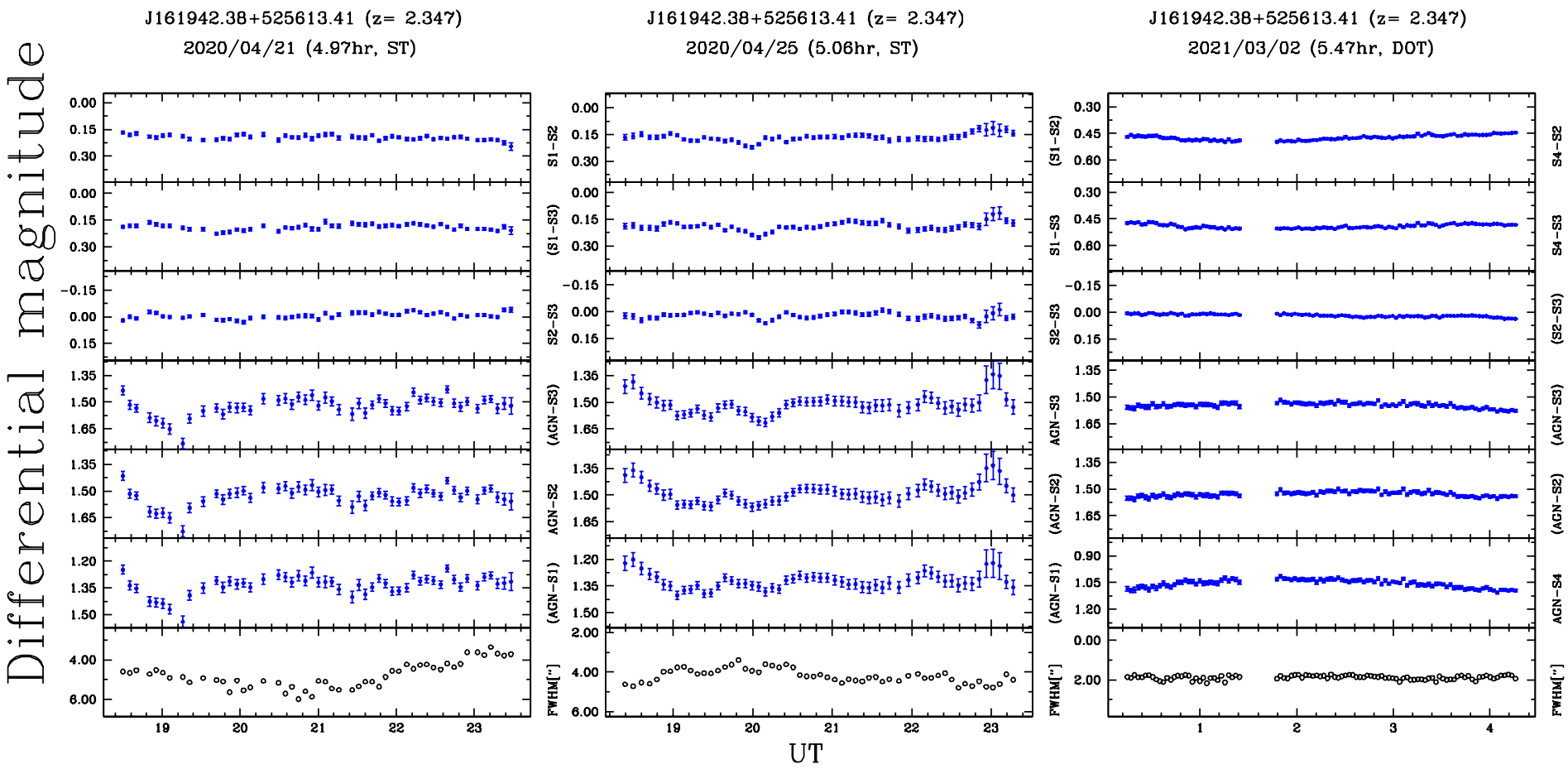

Figure 1: Differential light curves (DLCs) for the high-z FSRQ J161942.38+525613.41. The date and duration of the observation along with the name of the source J161942.38+525613.41 are given at the top of each night's data. The upper three panels give the comparison star–star DLCs, whereas the subsequent lower panels give the source–star DLCs as described by the labels on the right side. The bottom panel gives the variation in seeing during the course of observation.

results obtained from the F_η test, as shown in Table 2, indicate that J161942.38+525613.41 is PV during the first night, NV during the second one, and V during the last one. This seemingly non-obvious result may stem from a combination of factors, including the larger number of data points that could be measured in the same amount of time at the larger DOT than at the ST, as well as the smaller error bars at DOT.

The INOV variability amplitude (ψ, see Table 2, column (10)) was computed using the definition given by Heidt and Wagner (1996):

$$\psi = \sqrt{(A_{max} - A_{min})^2 - 2\sigma^2}.$$

Here A_{max} and A_{min} represent the maximum and minimum values in the source–star DLC and $\sigma^2 = \eta^2 \langle \sigma^2_{q-s} \rangle$, where σ^2_{q-s} is the root mean square (rms) error for the data points in the DLC and $\eta = 1.54$ is the scaling factor. The mean value of ψ for a session, i.e., the average of the ψ values estimated for the two selected DLCs of the target source, is given in column (10) of Table 2.

5. Discussion and Conclusion

In the *R*-band/*r*-band intranight monitoring reported in Chand et al. (2022), the observations for the two samples of high-z blazars correspond to their rest-frame UV emission. For the sources in their first sample (nine low-polarization FSRQs, $\mathrm{LP_{FSRQs}}$), the rest-frame wavelengths range from 1374 Å to 2078 Å (median 1973 Å), while for their second sample (five high-polarization FSRQs, $\mathrm{HP_{FSRQs}}$), the corresponding range is from 2078 Å to 2495 Å (median 2099 Å). The rest-frame wavelength of the high-z FSRQ J161942.38+525613.41, located at a redshift of 2.347, is 1914 Å, which makes it a suitable source for studying the intranight variability of UV emission.

Chand et al. (2022) estimated the duty cycle (DC) to be $\sim 30\,\%$ with $\psi > 3\,\%$ for the intranight variability of their nine $\mathrm{LP_{FSRQs}}$ at a median redshift of $z \simeq 2.25$. For their five $\mathrm{HP_{FSRQs}}$ at median redshift of $z \simeq 2.0$, the DC of intranight variability was estimated to be $\sim 12\,\%$ with $\psi > 3\,\%$. These results from an F_η test for nine $\mathrm{LP_{FSRQs}}$ and five $\mathrm{HP_{FSRQs}}$ are different from the past INOV estimates using the same F_η test on two counts. Firstly, Goyal et al. (2013a) estimated an INOV DC of $\sim 10\,\%$ for $\psi > 3\,\%$ cases, using a large sample of 12 moderately distant (median $z \simeq 0.7$) $\mathrm{LP_{FSRQs}}$ monitored in 43 intranight sessions of more than 4 h duration. In the same study, the INOV DC was found to be $\sim 38\%$ for $\psi > 3\,\%$ for a sample of 11 moderately distant (median $z \simeq 0.7$) $\mathrm{HP_{FSRQs}}$ monitored in 31 sessions. It is important to note that, based on these results, a strong correlation between INOV and p_{opt} was established for moderately distant blazars, despite the fact that the two sets of observations were made a decade apart. This suggests that the propensity of a given FSRQ to exhibit strong INOV is of a fairly stable feature and correlates tightly with the optical polarization class.

The DC of $\sim 30\,\%$ for high-z $\mathrm{LP_{FSRQs}}$ is considerably higher than that of their lower-z counterparts (DC $\simeq 10\,\%$) and is quite comparable to their lower-z $\mathrm{HP_{FSRQs}}$. The excess of DC found for high-z $\mathrm{LP_{FSRQs}}$ (DC $\simeq 30\,\%$) could possibly be even greater, considering that their

sample of $\mathrm{LP_{FSRQs}}$ is heavily biased towards the most luminous members of this AGN class, and variability is known to anti-correlate with luminosity according to several studies (e.g., Guo and Gu, 2014). However, it remains unknown whether the anti-correlation with luminosity is significant on the intranight time scales, as it has only been established for variability on month/year-like time scales so far. One possible explanation offered by Chand et al. (2022) for the high DC of $\mathrm{LP_{FSRQs}}$ is that some of their members are actually $\mathrm{HP_{FSRQs}}$ but were mistakenly categorized as $\mathrm{LP_{FSRQs}}$ since their observed polarization, p_{opt} (i.e., rest-frame UV polarization) may have been decreased due to dilution by thermal UV from the accretion disc.

Secondly, Chand et al.'s (2022) second sample of five $\mathrm{HP_{FSRQs}}$ did not support the above explanation. They estimated an INOV DC of $\sim 12\,\%$ for five $\mathrm{HP_{FSRQs}}$, which is quite low. These $\mathrm{HP_{FSRQs}}$ cannot be misidentified as $\mathrm{LP_{FSRQs}}$ since thermal dilution only lowers the polarization. Furthermore, Chand et al. (2022) looked for the observational biases (i.e., the intrinsic duration of monitoring and photometric sensitivity) that could have spuriously led to higher DC for $\mathrm{LP_{FSRQs}}$ compared to $\mathrm{HP_{FSRQs}}$. They found that the intrinsic duration of monitoring and photometric sensitivity for $\mathrm{LP_{FSRQs}}$ and $\mathrm{HP_{FSRQs}}$ is very similar, leading them to discard the possibility of observational biases. In summary, based on the results for nine $\mathrm{LP_{FSRQs}}$ and five $\mathrm{HP_{FSRQs}}$, a strong correlation of intranight variability of UV emission with polarization could not be found, in contrast to the strong correlation found for intranight variability of optical emission.

We now added three intranight observation sessions of the FSRQ J161942.38+525613.41 located at $z = 2.347$ to this intriguing result. It was monitored in R-band/r-band with a median duration of ~ 5 h using ST and DOT. Since the polarization information is unavailable in the literature, the FSRQ J161942.38+525613.41 could not be classified as $\mathrm{LP_{FSRQ}}$ or $\mathrm{HP_{FSRQ}}$. Therefore, it was included in both the samples of Chand et al. (2022) while estimating the INOV DC. For estimating the INOV DC, only the type 'V' sessions with confirmed variability of $\psi > 3\,\%$ were used. Only during one session (March 02, 2021 using DOT – see column (8) of Table 2) it was found to be variable ('V') with $\psi > 3\,\%$. A high DC of $\sim 30\,\%$ with $\psi > 3\,\%$ was estimated for the intranight variability of $\mathrm{LP_{FSRQs}}$ even after including the FSRQ J161942.38+525613.41 as a $\mathrm{LP_{FSRQ}}$. Similarly, when the source J161942.38+525613.41 was taken into account as a $\mathrm{HP_{FSRQ}}$, the estimated DC was found to be $\sim 16\,\%$ with $\psi > 3\,\%$ which is still fairly low. Thus, we found no evidence for a strong intranight variability of UV emission with polarization even after including the FSRQ J161942.38+525613.41 either as a low- or a high-polarization FSRQ, in contrast to the blazars monitored in the rest-frame blue-optical. This supports the proposal put forth in Chand et al. (2022) that the synchrotron radiation of blazar jets in the UV/X-ray regime arises from a relativistic particle population distinct from the one responsible for their synchrotron radiation up to near-infrared/optical frequencies. However, the measurement of polarization for the FSRQ J161942.38+525613.41 using the upcoming imaging polarimeter at the 3.6-m DOT will categorize the source as either $\mathrm{LP_{FSRQ}}$ or $\mathrm{HP_{FSRQ}}$, resulting in an increase of the size of one of two blazar samples of Chand et al. (2022) by just one unit, which is still small. The two blazar samples remain too small to be representative of the high-z blazar population, so the above finding might be spurious. Therefore, this interesting finding requires independent confirmation through intranight optical monitoring of a larger sample of high-z blazars with

both low and high polarization. Consequently, an enlarged sample of 34 high-z blazars was derived from the *Roma–BZCAT* catalogue to verify the above finding. We intend to observe it in the future using metre-class telescopes available in India (see Sects. 1 and 2).

Acknowledgments

We thank Prof. Paul J. Wiita for his valuable comments and suggestions for improving the quality of the manuscript. We thank the organisers for allowing us to present our work at the BINA conference and for the local support. We also thank Prof. Hum Chand for his thoughtful suggestions and discussion regarding the current work. The author also acknowledges the support of SERB-DST, New Delhi, for funding under the National Post-Doctoral Fellowship Scheme through grant no. PDF/2023/004071.

Further Information

Author's ORCID identifier

0000-0002-6789-1624 (Krishan CHAND)

Conflicts of interest

The author declares no conflict of interest.

References

Aharonian, F. A., Barkov, M. V. and Khangulyan, D. (2017) Scenarios for ultrafast gamma-ray variability in AGN. ApJ, 841(1), 61. https://doi.org/10.3847/1538-4357/aa7049.

Angelakis, E., Hovatta, T., Blinov, D., Pavlidou, V., Kiehlmann, S., Myserlis, I., Böttcher, M., Mao, P., Panopoulou, G. V., Liodakis, I., King, O. G., Baloković, M., Kus, A., Kylafis, N., Mahabal, A., Marecki, A., Paleologou, E., Papadakis, I., Papamastorakis, I., Pazderski, E., Pearson, T. J., Prabhudesai, S., Ramaprakash, A. N., Readhead, A. C. S., Reig, P., Tassis, K., Urry, M. and Zensus, J. A. (2016) RoboPol: the optical polarization of gamma-ray-loud and gamma-ray-quiet blazars. MNRAS, 463(3), 3365–3380. https://doi.org/10.1093/mnras/stw2217.

Bachev, R., Strigachev, A. and Semkov, E. (2005) Short-term optical variability of high-redshift quasi-stellar objects. MNRAS, 358, 774–780. https://doi.org/10.1111/j.1365-2966.2005.08708.x.

Blandford, R. D. and Rees, M. J. (1978) Extended and compact extragalactic radio sources: interpretation and theory. PhyS, 17, 265–274. https://doi.org/10.1088/0031-8949/17/3/020.

Bourda, G., Charlot, P., Porcas, R. W. and Garrington, S. T. (2010) VLBI observations of optically-bright extragalactic radio sources for the alignment of the radio frame with the future gaia frame. I. Source detection. A&A, 520, A113. https://doi.org/10.1051/0004-6361/201014248.

Cara, M., Perlman, E. S., Uchiyama, Y., Cheung, C. C., Coppi, P. S., Georganopoulos, M., Worrall, D. M., Birkinshaw, M., Sparks, W. B., Marshall, H. L., Stawarz, L., Begelman, M. C., O'Dea, C. P. and Baum, S. A. (2013) Polarimetry and the high-energy emission mechanisms in quasar jets: The case of PKS 1136-135. ApJ, 773(2), 186. https://doi.org/10.1088/0004-637X/773/2/186.

Chand, K. and Gopal-Krishna (2022) Persistence of the blazar state in flat-spectrum radio quasars. MNRAS, 516(1), L18–L23. https://doi.org/10.1093/mnrasl/slac066.

Chand, K., Gopal-Krishna, Omar, A., Chand, H., Mishra, S., Bisht, P. S. and Britzen, S. (2022) Intranight variability of ultraviolet emission from powerful blazars. MNRAS, 511(1), 13–18. https://doi.org/10.1093/mnrasl/slab129.

Chand, K., Gopal-Krishna, A., Omar, Chand, H. and Bisht, P. S. (2023) The transience and persistence of high optical polarisation state in beamed radio quasars. PASA, 40, e006. https://doi.org/10.1017/pasa.2023.3.

Condon, J. J., Cotton, W. D., Greisen, E. W., Yin, Q. F., Perley, R. A., Taylor, G. B. and Broderick, J. J. (1998) The NRAO VLA Sky Survey. AJ, 115(5), 1693–1716. https://doi.org/10.1086/300337.

Garcia, A., Sodré, L., Jablonski, F. J. and Terlevich, R. J. (1999) Optical monitoring of quasars – I. Variability. MNRAS, 309, 803–816. https://doi.org/10.1046/j.1365-8711.1999.02884.x.

Gopal-Krishna, Chand, K., Chand, H., Negi, V., Mishra, S., Britzen, S. and Bisht, P. S. (2023) Intranight optical variability of low-mass active galactic nuclei: a pointer to blazar-like activity. MNRAS, 518(1), L13–L18. https://doi.org/10.1093/mnrasl/slac125.

Gopal-Krishna, Sagar, R. and Wiita, P. J. (1995) Intranight optical variability in optically selected QSOs. MNRAS, 274, 701–710. https://doi.org/10.1093/mnras/274.3.701.

Gopal-Krishna and Wiita, P. J. (2018) Optical monitoring of Active Galactic Nuclei from ARIES. BSRSL, 87, 281–290.

Goyal, A., Gopal-Krishna, Wiita, P. J., Anupama, G. C., Sahu, D. K., Sagar, R. and Joshi, S. (2012) Intra-night optical variability of core dominated radio quasars: the role of optical polarization. A&A, 544, A37. https://doi.org/10.1051/0004-6361/201218888.

Goyal, A., Gopal-Krishna, Wiita, P. J., Stalin, C. S. and Sagar, R. (2013a) Improved characterization of intranight optical variability of prominent AGN classes. MNRAS, 435, 1300–1312. https://doi.org/10.1093/mnras/stt1373.

Goyal, A., Mhaskey, M., Gopal-Krishna, Wiita, P. J., Stalin, C. S. and Sagar, R. (2013b) On the photometric error calibration for the differential light curves of point-like Active Galactic Nuclei. JApA, 34(3), 273–296. https://doi.org/10.1007/s12036-013-9183-7.

Gregory, P. C., Scott, W. K., Douglas, K. and Condon, J. J. (1996) The GB6 catalog of radio sources. ApJS, 103, 427–432. https://doi.org/10.1086/192282.

Guo, H. and Gu, M. (2014) The optical variability of SDSS quasars from multi-epoch spectroscopy. I. Results from 60 quasars with $\geq$ six-epoch spectra. ApJ, 792(1), 33. https://doi.org/10.1088/0004-637X/792/1/33.

Heidt, J. and Wagner, S. J. (1996) Statistics of optical intraday variability in a complete sample of radio-selected BL Lacertae objects. A&A, 305, 42. https://ui.adsabs.harvard.edu/abs/1996A%26A...305...42H.

Impey, C. D. and Tapia, S. (1990) The optical polarization properties of quasars. ApJ, 354, 124–139. https://doi.org/10.1086/168672.

Jester, S., Meisenheimer, K., Martel, A. R., Perlman, E. S. and Sparks, W. B. (2007) Hubble Space Telescope far-ultraviolet imaging of the jet in 3C273: a common emission component from optical to X-rays. MNRAS, 380(2), 828–834. https://doi.org/10.1111/j.1365-2966.2007.12120.x.

Kumar, B., Omar, A., Maheswar, G., Pandey, A. K., Sagar, R., Uddin, W., Sanwal, B. B., Bangia, T., Kumar, T. S., Yadav, S., Sahu, S., Pant, J., Reddy, B. K., Gupta, A. C., Chand, H., Pandey, J. C., Joshi, M. K., Jaiswar, M., Nanjappa, N., Purushottam, Yadav, R. K. S., Sharma, S., Pandey, S. B., Joshi, S., Joshi, Y. C., Lata, S., Mehdi, B. J., Misra, K. and Singh, M. (2018) 3.6-m Devasthal Optical Telescope project: Completion and first results. BSRSL, 87, 29–41. https://doi.org/10.25518/0037-9565.7454.

Massaro, E., Maselli, A., Leto, C., Marchegiani, P., Perri, M., Giommi, P. and Piranomonte, S. (2015) The 5th edition of the *Roma-BZCAT*. A short presentation. Ap&SS, 357(1), 75. https://doi.org/10.1007/s10509-015-2254-2.

Moore, R. L. and Stockman, H. S. (1984) A comparison of the properties of highly polarized qsos versus low-polarization QSOs. ApJ, 279, 465–484. https://doi.org/10.1086/161911.

Omar, A., Kumar, T., Reddy, B., Pant, J. and Mahto, M. (2019) First-light images from low-dispersion spectrograph-cum-imager on 3.6 m Devasthal Optical Telescope. CSci, 116, 1472–1478. https://doi.org/10.18520/cs/v116/i9/1472-1478.

Peña-Herazo, H. A., Massaro, F., Gu, M., Paggi, A., Landoni, M., D'Abrusco, R., Ricci, F., Masetti, N. and Chavushyan, V. (2021) An optical overview of blazars with LAMOST. I. Hunting changing-look blazars and new redshift estimates. AJ, 161(4), 196. https://doi.org/10.3847/1538-3881/abe41d.

Punsly, B., Marziani, P., Zhang, S., Muzahid, S. and O'Dea, C. P. (2016) The extreme ultraviolet variability of quasars. ApJ, 830(2), 104. https://doi.org/10.3847/0004-637X/830/2/104.

Rakshit, S., Stalin, C. S. and Kotilainen, J. (2020) Spectral properties of quasars from Sloan Digital Sky Survey Data Release 14: The catalog. ApJS, 249(1), 17. https://doi.org/10.3847/1538-4365/ab99c5.

Sagar, R. (1999) Some new initiatives in optical astronomy at UPSO, Nainital. CSci, 77, 643–652.

Sagar, R., Stalin, C. S., Gopal-Krishna and Wiita, P. J. (2004) Intranight optical variability of blazars. MNRAS, 348, 176–186. https://doi.org/10.1111/j.1365-2966.2004.07339.x.

Stalin, C. S., Gopal-Krishna, Sagar, R. and Wiita, P. J. (2004) Intranight optical variability of radio-quiet and radio lobe-dominated quasars. MNRAS, 350, 175–188. https://doi.org/10.1111/j.1365-2966.2004.07631.x.

Stetson, P. B. (1987) DAOPHOT – A computer program for crowded-field stellar photometry. PASP, 99, 191–222. https://doi.org/10.1086/131977.

Stetson, P. B. (1992) More experiments with DAOPHOT II and WF/PC images. In Astronomical Data Analysis Software and Systems I, edited by Worrall, D. M., Biemesderfer, C. and Barnes, J., vol. 25 of *ASPC*, pp. 297–306. https://ui.adsabs.harvard.edu/abs/1996ApJS..103..427G.

Stockman, H. S., Moore, R. L. and Angel, J. R. P. (1984) The optical polarization properties of "normal" quasars. ApJ, 279, 485–498. https://doi.org/10.1086/161912.

Uchiyama, Y., Urry, C. M., Cheung, C. C., Jester, S., Van Duyne, J., Coppi, P., Sambruna, R. M., Takahashi, T., Tavecchio, F. and Maraschi, L. (2006) Shedding new light on the 3C 273 jet with the Spitzer Space Telescope. ApJ, 648(2), 910–921. https://doi.org/10.1086/505964.

Uchiyama, Y., Urry, C. M., Coppi, P., Van Duyne, J., Cheung, C. C., Sambruna, R. M., Takahashi, T., Tavecchio, F. and Maraschi, L. (2007) An infrared study of the large-scale jet in quasar PKS 1136-135. ApJ, 661(2), 719–727. https://doi.org/10.1086/518089.

Urry, C. M. and Padovani, P. (1995) Unified schemes for radio-loud Active Galactic Nuclei. PASP, 107, 803–845. https://doi.org/10.1086/133630.

Wagner, S. J. and Witzel, A. (1995) Intraday variability in quasars and BL LAC objects. ARA&A, 33, 163–198. https://doi.org/10.1146/annurev.aa.33.090195.001115.

Wills, B. J., Wills, D., Breger, M., Antonucci, R. R. J. and Barvainis, R. (1992) A survey for high optical polarization in quasars with core-dominant radio structure: Is there a beamed optical continuum? ApJ, 398, 454–475. https://doi.org/10.1086/171869.

Xin, C., Charisi, M., Haiman, Z. and Schiminovich, D. (2020) Correlation between optical and UV variability of a large sample of quasars. MNRAS, 495(1), 1403–1413. https://doi.org/10.1093/mnras/staa1258.